

doi:

# Numerical Analysis of Aerodynamic Compensation Pitot-Static Tube

Tanja Žunić<sup>1)</sup>  
 Biljana Dovatov<sup>1)</sup>  
 Ilija Nenadić<sup>1)</sup>

Numerical analysis of a flow field around the aerodynamic compensation pitot-static tube that is used on a domestic ORAO J-22 aircraft is presented in this paper. The analysis was performed for three different Mach numbers of the free stream velocity for two configurations of the pitot-static tube. The comparison of the pressure coefficient ( $C_p$ ) distribution for both of the configurations is given.

*Key words:* pitot-static tube, aerodynamic compensation, CFD analysis, roughness, transonic, pressure coefficient.

## Introduction

THE pitot-static tube (pitot tube) is one of the most important air data sensors and is designed to measure ambient static and total pressure corresponding to the flight conditions. These pressure values are translated into aircraft speed, altitude, Mach number, vertical speed, and are necessary for the functioning of multiple aircraft systems such as flight control systems, avionics, cockpit flight instruments, etc. Correct measurement of the ambient static pressure through the whole range of Mach numbers (subsonic and supersonic) is the most demanding aspect in its design [1]. One of the most difficult tasks is the accurate determination of static pressure at transonic speeds. The position and shape of pitot tube that are satisfying at subsonic speeds are usually not suitable at transonic speeds, where the pressure changes in the disturbed (affected) field are sudden and significant. An "aerodynamic-compensation" pitot tube has been designed to "compensate" position error by generating an opposite local pressure coefficient,  $C_p$  [2-4]. The shape of this type of pitot tube is illustrated in Fig.1. A common aerodynamic compensation pitot tube has an ogival shape whose profile is defined by a quadratic polynomial.

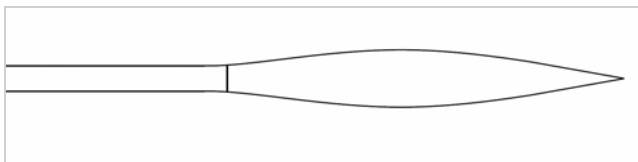


Figure 1. Aerodynamic compensation pitot-static tube with ogival shape

The available literature on this topic is mostly limited to NACA reports from the 1950s. Therewith, a group of the profesores and students at the Air University in Pakistan, recently published a couple of manuscripts regarding this topic [5-6]. They used CFD analysis to determine the ogivale profile of the pitot tube in order to achieve the desirable

pressure coefficient for both regimes, subsonic and supersonic. They also used the same method to analyze the performance characteristics of pressure based flush angle-of-attack measurement system, integrated on a pitot-static tube.

This type of pitot tube is used on the domestically produced aircraft, ORAO J-22, Fig.2. It was made according to the Chaffois 40-400 model made by French manufacturer Badin-Crouzet [7], Fig.3. The tube has an ogival shape with maximum diameter of 40 mm and length of 500 mm. A rough surface ring is placed at 55 mm from the beginning of the probe, 12 mm wide [8].



Figure 2. Pitot tube on ORAO J-22 aircraft

The aim of the present study is the numerical analysis and representation of the flow field around the pitot tube in different flow conditions. The concept for this study originated from an assignment which required the analysis of the flow field around the modified ORAO aircraft and the influence of the modifications on the flow field around the pitot tube. It was not possible to find the experimental data in

<sup>1)</sup> Military Technical Institute (VTI), Ratka Resanovića 1, 11132 Belgrade, SERBIA  
 Correspondence to: Tanja Žunić; e-mail: tazunic7@gmail.com

the available literature for this type of pitot tube, so the study will only regard numerical analysis.

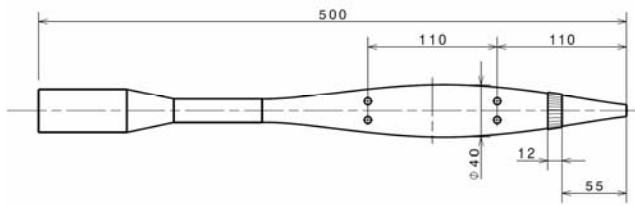


Figure 3. Chaffois 40-400 pitot-static tube [6]

### Numerical model

The geometry of the pitot tube is axisymmetric along its longitudinal axis, so a 3D half modeling was done for CFD analysis. The computational domain included the free stream far field, pitot tube, the symmetry axis and body of influence around pitot tube. Fig.4 shows the computational domain and position of the tube relative to the domain.

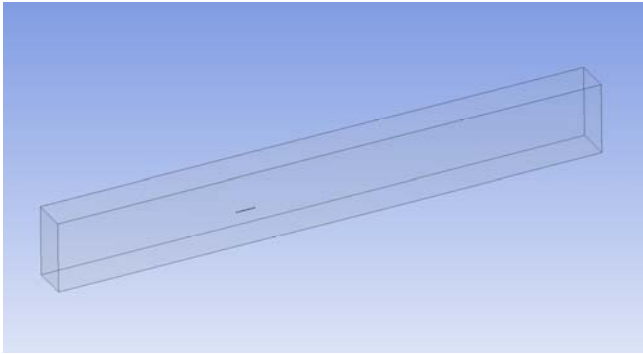


Figure 4. Computational domain

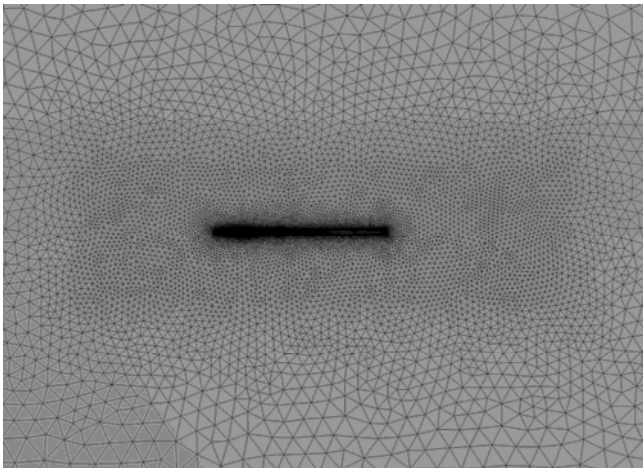


Figure 5. Computational mesh of body of influence

Analyses were performed on an unstructured mesh with 15 layers of thin prismatic cells around the pitot tube in order to capture flow changes in the vicinity of the model. The growth rate of the body of influence's cells were reduced in the same manner, Fig.5. The computational mesh near the pitot tube surface is shown in Fig.6. In this configuration, the mesh has around 3 million cells.

CFD calculations presented in this article were performed in commercial ANSYS Fluent software by the finite volume method. The Reynolds Average Navier Stokes system of equations were solved for 3D compressible flow using density-based solver with implicit formulation of Fluent. Spatial discretization set up was kept by default settings. The

default parameters were used during defining the spatial discretization. Two turbulent models were used: the one-equation Spalart-Allmaras (S-A) and the two-equation  $k-\omega$  SST. The working fluid is defined as air with ideal gas characteristics at sea level.

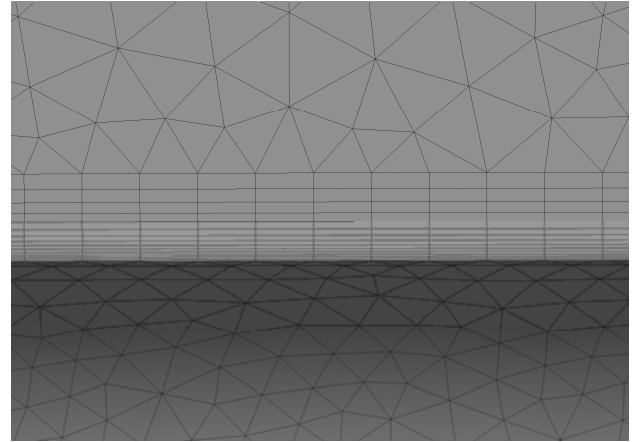


Figure 6. Details of mesh in the vicinity of the pitot tube surface

Pressure far field boundary conditions were used for defining the free stream far field. At the surface of the pitot tube, a no-slip wall boundary condition was applied, whereas a rough wall boundary condition was used at the ring in front of the pitot tube area, with a 0.5 mm roughness height. A symmetry boundary condition was specified at the symmetry axis. The computations were performed until the convergence criteria were achieved.

### Results

In the present analysis, computations were performed for three different Mach numbers: 0.5, 0.8 and 1.1. The three characteristic Mach numbers were chosen in order to cover relevant air speeds of the ORAO aircraft which occur during subsonic and transonic flight. Two configurations were simulated: one with a rough ring on pitot tube and other with a smooth ring on the pitot tube. In all the cases of the present study the flow field consists of a free stream flow with distinct changes in the area around the pitot tube, which later merges with the free stream flow far away from the pitot tube. Therefore, only the flow field around the pitot tube will be shown for all cases.

The comparison of the velocity contours around the model obtained by mentioned turbulent models (S-A and  $k-\omega$  SST) is shown in Figures 7 - 9. At Mach 0.5 for the free stream velocity, the velocity contours are almost identical for both of the turbulent models. The same pattern can be noticed at Mach 1.1, Fig.9. For Mach 0.8 this is not the case, where obvious differences in the velocity contours can be noticed between the two models, especially in the zone of the pitot tube's maximum diameter, Fig.8. This is caused by the limitations of the S-A model in the turbulent flow regimes with increased viscosity.

The variation of the pressure coefficient  $C_p$  along the surface of the pitot tube "compensation" region, obtained by the  $k-\omega$  SST model, is shown in Figures 10 - 12. The longitudinal coordinates of the pitot tube along its axis are presented on the horizontal axis and the pressure coefficient values on the vertical axis. The figures shown present the distribution of the pressure coefficient that is enclosed only by the "compensation" region. The compensation region starts at 200 mm from the origin point and ends at 450 mm from the aforementioned point.

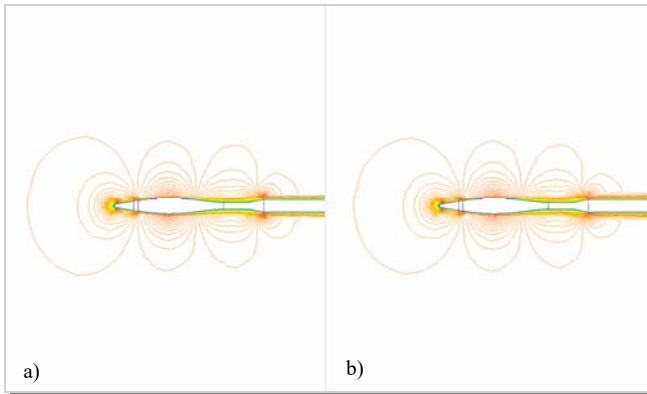


Figure 7. Velocity field at Mach 0.5: a) k- $\omega$  SST b) Spalart-Allmaras

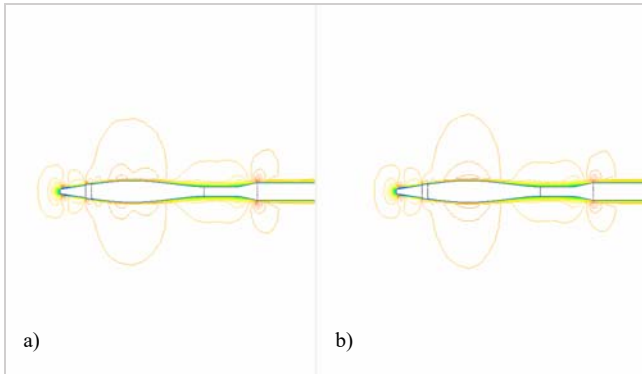


Figure 8. Velocity field at Mach 0.8: a) k- $\omega$  SST b) Spalart-Allmaras

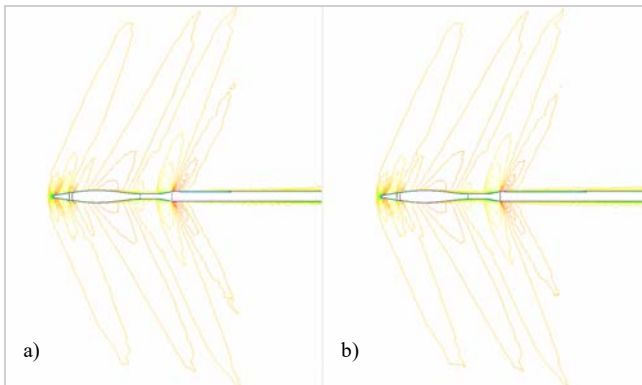


Figure 9. Velocity field at Mach 1.1: a) k- $\omega$  SST, b) Spalart-Allmaras

The results of the variations of the pressure coefficient obtained by k- $\omega$  SST model for the simulated configurations show the influence of the rough surface ring at Mach 0.8. At the other two Mach numbers, 0.5 and 1.1, the  $C_p$  variations are very close with small differences for both of the configurations, Figures 10 and 11. Usage of the rough ring in non-transonic regimes did not impact the results significantly along the compensation region.

Fig. 12 shows the pressure coefficient variation at Mach 0.8 for both of the configurations. The differences between the two configurations are very noticeable. Analyzing the  $C_p$  distribution, it can be noticed that having a rough ring placed in front of the measuring area “reduces” turbulent flow in contrast to the smooth ring at the same value of the free stream velocity.

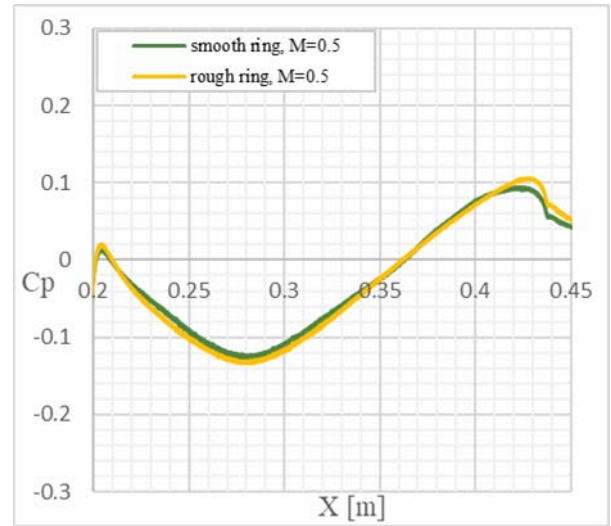


Figure 10. Distribution of the pressure coefficient at Mach 0.5

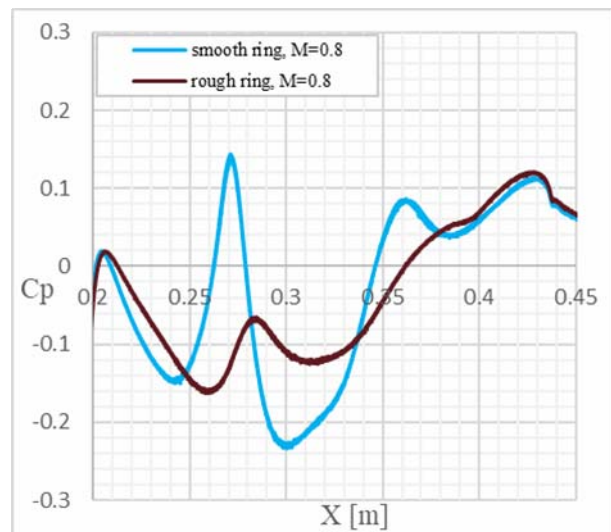


Figure 11. Distribution of the pressure coefficient at Mach 0.8

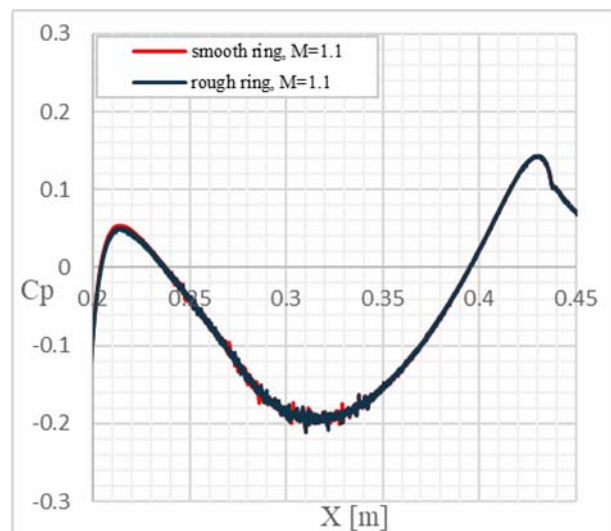


Figure 12. Distribution of the pressure coefficient at Mach 1.1

## Conclusion

In this paper numerical analysis of the flow field around the aerodynamic compensation pitot tube in different flow conditions is presented. Two configurations were analyzed: one with the rough ring on the pitot tube and one with the smooth ring on the pitot tube in other case. The pressure coefficient distribution was obtained using the  $k-\omega$  SST turbulent model. The comparison of the results at Mach 0.8 shows significant differences between the two configurations. In this case, a rough ring placed in front of the measuring area, the “compensated” region, reduces the pressure coefficient. In future, it would be desirable to perform wind tunnel tests as well as to analyze a wider range of Mach numbers with different configurations in a manner which will adequately determine the pressure and velocity distributions at critical flow conditions.

## References

- [1] GARCY, W.: *Measurement of aircraft speed*, NASA Reference Publication 1046, 1980
- [2] RICHIE, V.S.: *Several methods for aerodynamic reduction of static pressure sensing errors for aircraft at subsonic, near-sonic, and low supersonic speeds*, NASA TR R-18, 1959
- [3] LETKO, W.: *Investigation of the fuselage interference on a pitot-static tube extending forward from the nose of the fuselage*, NASA-TN-1496, 1947
- [4] O'BRYAN, T.C., DANFORTH, E.C.B., JOHNSTON, J.F.: *Error in airspeed measurement due to the static-pressure field ahead of an airplane at transonic speeds*, National Advisory Committee for Aeronautics R-1239, 1955
- [5] LATIF, A., MASUD, J., SHEIKH, S.R., PERVEZ, K., QAZI, O.A., QURESHI, H.: *Novel aerodynamic compensation pitot-static tube for application in subsonic and supersonic flight regimes*, 44<sup>th</sup> AIAA Aerospace Sciences Meeting and Exhibit, 2006
- [6] MASUD, J.: *Performance characteristics of flush angle-of-attack measurement system integrated on a pitot tube*, Engineering Applications of Computational Fluid Mechanics, 2010
- [7] WUEST, W.: *Pressure and flow measurement*, Advisory group for aerospace research and development, 1980
- [8] Federal Secretariat of People's Defense, Description and maintenance of the aircraft J-22 remaining installations (in Serbian), Belgrade 1991

Received: 09.06. 2023.  
Accepted: 01.09. 2023.

# Numerička analiza pito-statičke cevi sa „aerodinamičkom korekcijom”

U ovom radu prikazana je numerička analiza strujnog polja oko pito cevi sa „aerodinamičkom korekcijom” koja se koristi na avionu domaće proizvodnje, ORAO J-22. Analiza je vršena pri tri različita Mahova broja neporemećene struje vazduha za dve konfiguracije modela. Prikazana su poređenja raspodele koeficijenta pritiska ( $C_p$ ) za obe ispitane konfiguracije.

*Ključne reči:* pito-statička cev, aerodinamička kompenzacija, CFD analiza, hrapavost, transonika, koeficijent pritiska.